COMPACT NESTED APLANATIC OPTICS FOR CONCENTRATOR PHOTOVOLTAICS

Alex Goldstein[1], Daniel Feuermann[1], Gary Conley[2] and Jeffrey M. Gordon[1]

[1] Institute for Dryland Environmental Research, Ben-Gurion University of the Negev, Israel

[2] SolFocus, Mountain View, CA, USA

1. Introduction

Aplanatic optics were originally invented for improved imaging of telescopes and microscopes (Schwarzschild, 1905). Recently, these optics were considered for compact solar concentrators to be used in photovoltaic concentrator (CPV) designs (Gordon and Feuermann, 2005). Compactness is of paramount importance as it reduces manufacturing and shipping costs substantially. However, the two-mirror system – in the compact version of the design – causes shading of the primary mirror by the secondary and limits the level of practically achievable concentrations and/or forces the focus to be placed *inside* the optic. Passive cooling of the solar cell from within the optics (ruling out active cooling, for practical and economic reasons) is problematic as a large cooling fin (the size of roughly the aperture) in contact with ambient air is required for passive cooling. Thus, either a terminal dielectric concentrator to extract the concentrated sunlight into the solar cell located behind the primary mirror (Fig. 1) or a conical heat-conducting cone is necessary to permit positioning of the heat sink *behind* the primary from where heat can be rejected passively to the environment. It turns out that the heat-conducting cone is problematic causing relatively large temperature gradients along the cone and with it a relatively high temperature of the cell with the concomitant reduction in cell efficiency. Though the dielectric element does the job of extracting the light to the cell quite well, in fact permitting further concentration, there is the need for an optical bond to the cell without which additional Fresnel losses and totally internal reflected rays at the dielectric-air interface would result in intolerable losses. This optical bond has to withstand temperature variation and moisture over at least 20 years, a feat not easily achieved and of significant conern to the manufacturers. Nevertheless, the design of figure 1 has in fact been adopted for large-scale CPV systems and successfully deployed (Fig. 2, SolFocus, 2008-2011).

Is there an optic that could satisfy the constraints of compactness, low self shading, and avoiding a dielectric tertiary concentrator and bond while still being reasonably simple to manufacture? In this paper we suggest to nest the dual-mirror aplanats (akin to a Fresnel lens) that can satisfy all these objectives. We present two possibilities for which the optical performance was evaluated via ray trace simulations.

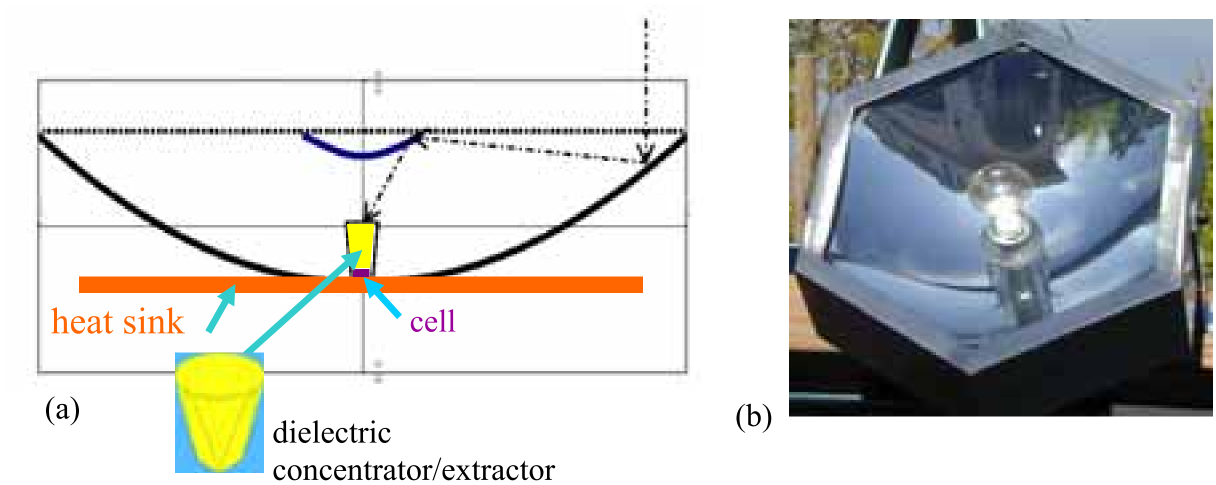

Fig. 1. a) Cross-section of the aplanatic concentrator; the compactness is expressed by the aspect ratio (AR), in this case AR=0.25; geometric concentration 625; shading 3.5%. A tapered dielectric element extracts the light and is optically bonded to a solar cell. b) completed prototype.

Fig. 2. Example of CPV deployment of aplanatic optic concentrators. The large number of modules on each tracker require accurate alignment of the individual modules and a stiff construction to have each element pointing in the same direction (SolFocus, 2010).

2. Maximum concentration and optical tolerance

A second (and no smaller) issue is the level of concentration, and, related to it, the acceptance angle function of the device. Given that the modern high-concentration, high-efficiency solar cells are not very sensitive to the homogeneity of the flux distribution on the solar cell (Katz et. al., 2006), the cell may be 'oversized' reducing the burden of accurate tracking and/or stiffness of the large modules typically mounted on a single dual-axis tracker (Fig. 2). This can be expressed in terms of tolerance to off-axis orientation (Gordon et. al., 2008, Goldstein and Gordon, 2011). For geometric concentration C_g (ratio of entry to active cell area), the deviation angle $\theta_{\text{off-axis}}$ up to which collection remains undiminished relative to on-axis performance is bounded by

$$\theta_{off-axis} \leq \frac{NA_{out}}{\sqrt{C_g}} - \theta_{sun} \qquad \text{(eq. 1)}$$

where NA = sin(θ) and NA_{out} is the exit numerical aperture, based on the largest angle of rays on the cell surface. (The current CPV convention defines optical tolerance as the angular deviation up to which 90% of on-axis collection is maintained.) Accordingly, CPV optics are typically designed with C_g well below C_{max}. The relationship between the numerical aperture and maximum concentration (permitted by thermodynamics) is given by (Winston et. al, 2008)

$$C_{\max} = \left(\frac{\sin(\theta_{out})}{\sin(\theta_{in})}\right)^2 = \left(\frac{NA_{out}}{NA_{in}}\right)^2 \qquad \text{(eq. 2)}$$

where NA_{in} is the input numerical aperture (typically, a convolution of the sun angle and the optical quality of the optics (Rabl, 1985)). An example of an aplanat design with high NA_{out}, high concentration, device is shown in Figure 3 exemplifying the problematic of passive cooling of the cell. Here and in subsequent illustrations we note that: (a) the scale is set by defining the focal length as unity, for which the diameter of the primary mirror equals $2NA_{out}$, and (b) the mirror contours follow from selecting the two parameters s (the separation of the vertices of the primary and secondary mirrors) and K (the separation of the secondary vertex and the focus). Aplanatism calls for every ray from the paraxial incident wave front satisfying both constant optical path length and the Abbe sine condition. The mirror contours have closed-form solutions (Gordon and Feuermann, 2005).

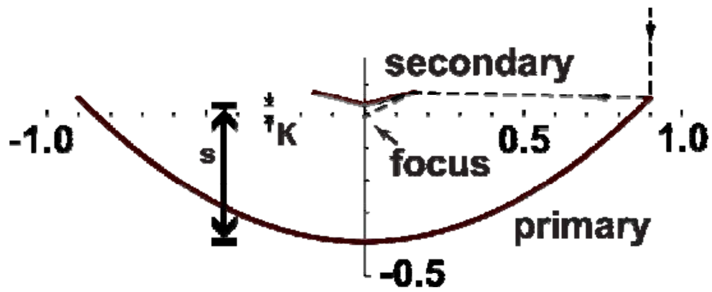

Fig 3. Example of an ultra-compact (aspect ratio *AR* = 0.259, i.e., ratio of depth to diameter), dual-mirror aplanat of high exit numerical aperture (NA_{out} = 0.9) and low shading of the primary by the secondary mirror (3.5%), but requiring the focus inside the optic. K and s are parameters representing the distance between the vertex of the secondary mirror and the focus, and the distance between the vertices of the two mirrors. One on-axis ray is traced for clarity.

In the following section we present solutions that overcome the above mentioned limitation. Aiming for high concentration and collection efficiency, we chose (a) 0.9 as the largest NA_{out} value in consideration of the angular dependence of reflective losses off solar cell surfaces (Spectrolab, 2009), (b) shading losses below 4%, (c) ray rejection not exceeding 4% (established with ray tracing) and (d) $AR < 0.3$ (the basic bound being $AR \geq 0.25$ (Winston and Gordon, 2005).

3. Nested aplanat design formalism

The inability of the aplanatic dual-mirror formalism to produce an external focus with large NA_{out} (i.e., large concentration) in a compact, low-shading optics prompts the search for an extra degree of freedom. A key realization is that the area above the secondary in the aplanat of Fig. 1a could be used to nest another nominally independent co-axial dual-mirror aplanat, as illustrated in Fig. 4. This allows the original (now outer) aplanat to be designed with a far larger secondary (relative to its primary), which in turn permits the focus to be located outside the optic.

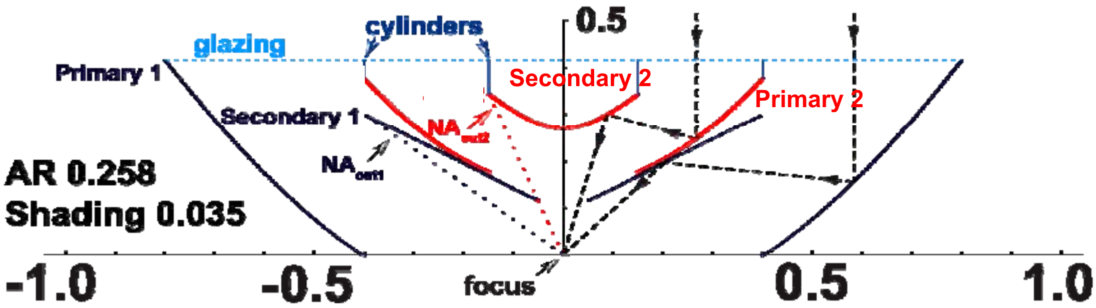

Fig. 4. Concentrator optics constructed of two nested aplanats. The two distinct aplanats here are characterized by {s_1 = 0.25, K_1 = 0.1035}, {s_2 = 0.125, K_2 = 0.27} and NA_{out2} = 0.4. NA_{out} = 0.8 is the highest value (and hence determines the concentration). This design has been optimized to maintain shading losses below 4% while respecting ultra-compactness and an external focus. Two rays are traced for clarity. The vertical lines (in blue) indicate thin cylindrical sections that permit attachment of the mirror sections to the top glazing.

The exit NA of the inner aplanat (NA_{out2}) is taken as the largest value consistent with avoiding shading from the outer aplanat (the exit NA of the latter, NA_{out1}, establishes the overall NA_{out}). The actual shading loss then stems exclusively from the inner aplanat, and can be maintained as low as a few percent. Toward facilitating manufacturability, the intermediate element is mirrored on both sides and serves double duty as both the primary for the inner aplanat and the secondary for the outer aplanat. The cylindrical sections – connecting the mirror contours with the glazing which is taken as a base to minimize tolerance build-up – can be kept thin enough so as not to cause shading losses exceeding a per cent or so. Figure 5 shows a tolerance graph for the aplanat of Figure 4 and is obtained by ray trace simulation. Ray rejection, shading, and blocking have been accounted for. The choice of geometrical concentration ratios C_g is obtained by choosing the cell size. The dashed vertical lines indicate the respective theoretical limits on tolerance angle (Eq. (1)), meaning the off-axis half-angle up to which 100% of the on-axis efficiency could be retained. The X symbols indicate ray trace results for the respective optical tolerances actually realized for 90% of on-axis collection.

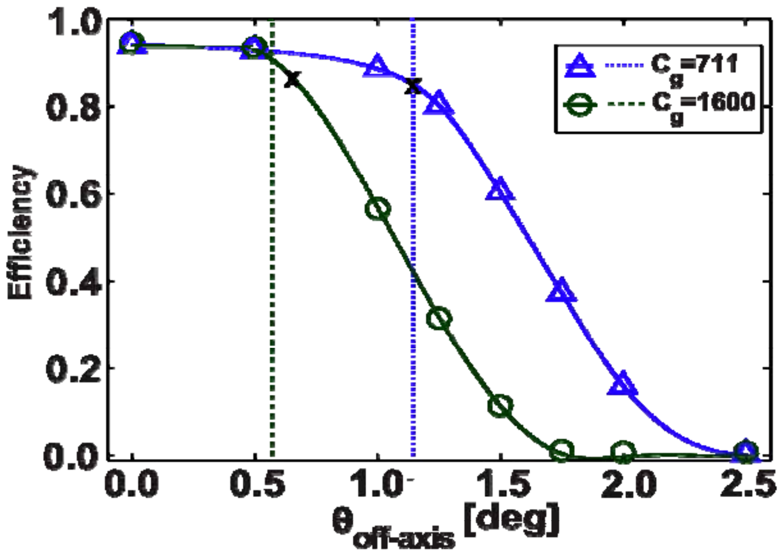

Fig 5. Optical tolerance plot for the concentrator of figure 4 with C_g = 711 and 1600. Efficiency refers to *geometric* collection efficiency, which accounts for shading, blocking and ray rejection (beyond absorptive and reflective losses that are case-specific and readily accounted for separately).

The nesting concept can be continued *ad infinitum*, but is illustrated here for only one additional aplanat (Fig. 6) in light of the perceived practicality of manufacture and for clarity of illustration. (Note that the optic always incurs precisely two mirror reflections independent of the number of nested aplanats.) Designing from the outside (aplanat 1) inward, and referring to Fig 6, one determines the highest value of NA_{out2} which incurs no self-shading of primary 1 by secondary 1, and still maintains an external focus. This condition establishes the highest achievable $NA_{out1} = NA_{out}$. Aplanats 2 and 3 are then determined by minimizing overall shading, while requiring low AR. In fact, the extra degree of freedom introduced by the additional nested aplanat allows NA_{out} to be increased to 0.9, while lowering shading to below 2% and still maintaining AR below 0.3.

The nested designs presented here were compared against the best corresponding conventional dual-mirror aplanats (similar to the one shown in Figure 1) and, via raytrace simulation, were found to provide the same near-maximum performance of high flux concentration at high efficiency (Gordon and Feuermann, 2005; Oustromov et. al., 2009).

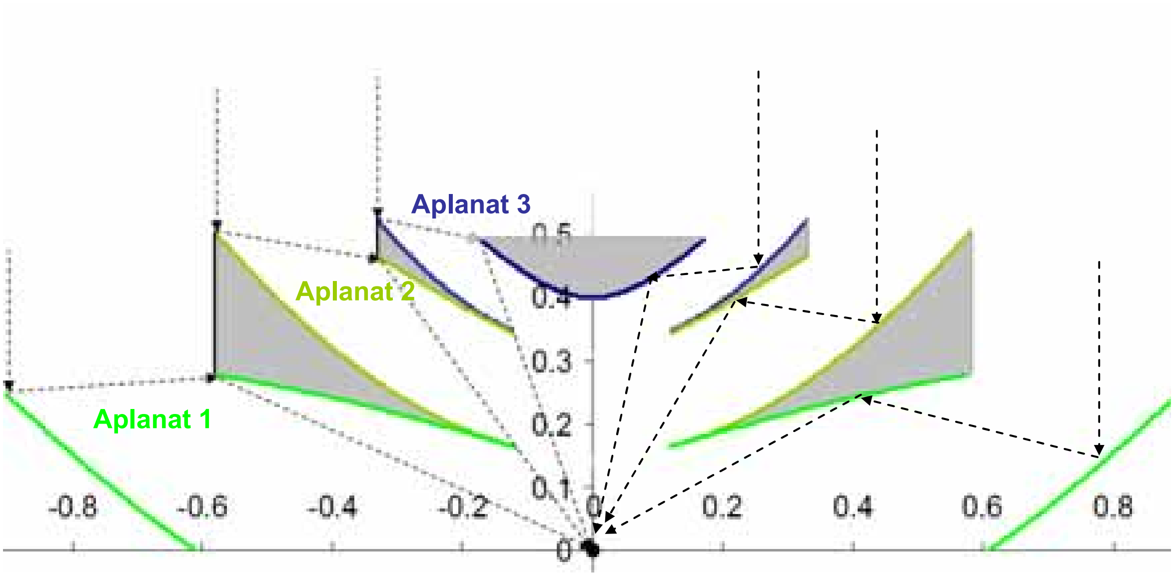

Fig. 6. Triple-nested aplanat. Notation as in Fig. 4. Aspect ratio is AR=0.277 and shading is 1.8%. The 3 distinct aplanats are characterized by {s_1 = 0.315, K_1 = 0.0625}, {s_2 = 0.143, K_2 = 0.2}, {s_3 = 0.0705, K_3 = 0.3} with NA_{out3} = 0.3, NA_{out2} = 0.573, and NA_{out1} = NA_{out} = 0.9. The intermediate elements are mirrored on both sides, each manufactured as a single element, with the upper contour serving as a primary and the underside as a secondary mirror. The uppermost mirror element (in this instance, intermediate primary 2) attaches directly to a protective entry glazing, with the remainder of the mirrors being attached via minimally-obstructive cylinders.

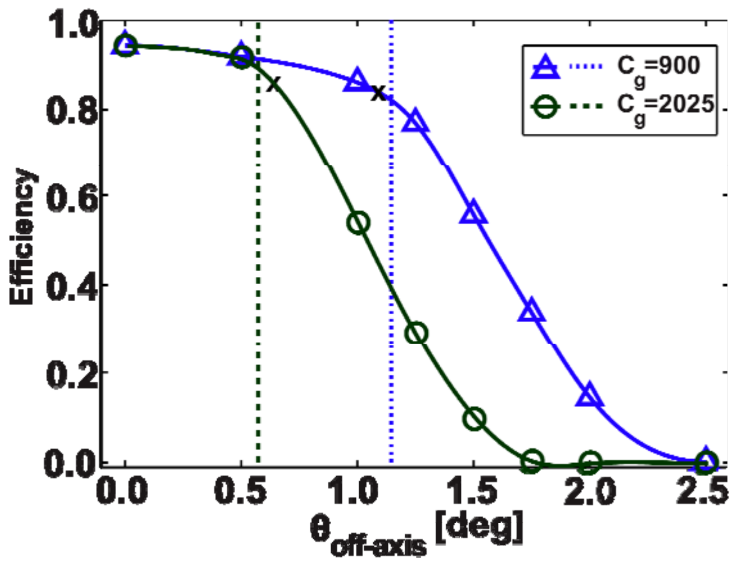

Fig. 7. Optical tolerance plots for C_g = 900 and 2025. Labels as in Fig. 5.

4. Conclusions

The strategy of nesting dual-mirror aplanats for high-efficiency, high-tolerance solar concentration surmounts the previously perceived limitation of precluding placement of the absorber *outside* the optic while retaining ultra-compactness (aspect ratios below 0.3) at low shading loss (< 4%). It thereby obviates the need for dielectric terminal concentrators and the associated optical bond to the solar cell. Having each intermediate component simultaneously fulfill two functions - with an upper surface that is a primary mirror for an interior aplanat and a lower side that is a secondary mirror for an exterior aplanat - facilitates manufacturability and minimizes losses due to shading and blocking. Furthermore, each mirror component can be produced as a cone-shaped element connected to a straight cylinder that attaches to a module's entry glazing, for tractable precision alignment.

For realistic optical errors (effective solar input angle of 10 mrad) and for concentration values characteristic of current and near-term CPV systems (from ~700 to 2000), double- and triple-nested aplanats were found to deliver the optical tolerance, collection efficiency and flux concentration of their single-aplanat predecessors (all close to their respective fundamental limits), but without the latter's need for extractors and optical bonds. The nested-aplanat concept could also be used in reverse (i.e., for maximum-performance collimation) in illumination applications.

References

Goldstein, A., and J.M. Gordon, 2011. Tailored solar optics for maximal optical tolerance and concentration, Sol. Energy Mater. Sol. Cells 95: 624-629.

Gordon, J. M. and D. Feuermann, 2005. Optical performance at the thermodynamic limit with tailored imaging designs, *Applied Optics*, Vol 44 pp. 2326-2331.

Gordon, J. M., D. Feuermann, and P. Young, 2008. Unfolded aplanats for high-concentration photovoltaics, Opt. Lett. 33:1114-1116.

Katz, E. A., J. M. Gordon and D. Feuermann, 2006. Effects of ultra-high flux and intensity distribution in multi-junction solar cells. *Progress in Photovoltaics*: Research and Applications, v**.** 14, No.4, p. 297 -303.

Ostroumov, N., J.M. Gordon, and D. Feuermann. 2009. Panorama of dual-mirror aplanats for maximum concentration, Appl. Opt. 48:4926-4931.

Rabl, A. 1985. Active solar collectors and their applications. Oxford University Press.

Schwarzschild, K., 1905. Untersuchungen zur geometrischen Optik I-III, Abh. Königl. Ges. Wis. Göttingen, Math-phys. Kl. 4, Nos. 1-3 (1905-1906).

SolFocus Inc., 2008-2011. 510 Logue Ave., Mountain View, CA 94043, personal communications and company technical reports.

Spectrolab Inc. 2009. Technical prospectus CDO-100-C3MJ, 12500 Gladstone Ave., Sylmar, CA 91342.

Winston, R. and J.M. Gordon, 2005. Planar concentrators near the étendue limit, Opt. Lett. 30 (2005) 2617-2619.

Winston, R., J.C. Miñano, P. Benítez, with contributions from N. Shatz, J. Bortz, 2008. Nonimaging Optics, Elsevier, Oxford (2008).